

PHYSICAL LAYER ABSTRACTION FOR PERFORMANCE EVALUATION OF LEO SATELLITE SYSTEMS FOR IOT USING TIME-FREQUENCY ALOHA SCHEME

Sylvain Cluzel^{*‡}, Mathieu Dervin[¶], José Radzik[‡], Sonia Cazalens[§]
Cédric Baudoin[¶] and Daniela Dragomirescu[†]

^{*‡}Laboratoire TésA, Toulouse – sylvain.cluzel@tesa.prd.fr [†]INSA-LAAS/CNRS, Toulouse – daniela@laas.fr

[‡]ISAE-SUPAERO, Université de Toulouse, France – jose.radzik@isae.fr

[§]Centre National d'Études Spatiales, Toulouse – sonia.cazalens@cnes.fr

[¶]Thales Alenia Space, Toulouse {cedric, mathieu}. {baudoin, dervin} @thalesaleniaspace.com

ABSTRACT

One of the main issues in using a Low Earth Orbit (LEO) satellite constellation to extend a Low-Powered Wide Area Network is the frequency synchronization. Using a link based on random access solves this concern, but also prevents delivery guarantees, and implies less predictable performance. This paper concerns the estimation of Bit Error Rate (BER) and Packet Error Rate (PER) using physical layer abstractions under a time and frequency random scheme, namely Time and Frequency Aloha. We first derive a BER calculation for noncoded QPSK transmission with one collision. Then, we use the 3GPP LTE NB-IoT coding scheme. We analyze the interference that could be induced by repetition coding scheme and propose an efficient summation to improve the decoder performance. Finally, to estimate a PER for any collided scenario, we propose a physical layer abstraction, which relies on an equivalent Signal-to-Noise Ratio (SNR) calculation based on Mutual Information.

Index Terms— Satellite, NB-IoT, LPWAN, Time-Frequency Aloha, Mutual information

1. INTRODUCTION

Low Powered Wide Area Networks (LPWAN) [1] for Internet of Things (IoT) communications is a growing market. LPWAN network operators try to outperform competition by having the widest coverage. Using a Low-Earth Orbit (LEO) satellite system to extend a LPWAN coverage is an attractive option, and has already been proposed [2, 3]. These solutions rely on random access protocols, both in the time and the frequency domains. The time randomness is inherent in state of the art LPWAN solutions, because leading market technologies (Sigfox, LoRa) use plain Aloha [4]. Additionally, when using a LEO satellite system, the channel suffers from Doppler shift. As carrier frequency offset compensation is too complex to be used with low-cost terminals, we consider the transmission frequency as random, so the compensation is not needed.

This leads to model the channel access as random both in the time and frequency domains. This subject has been studied under the name of Time-Frequency Aloha (TFA), or Time and Frequency Asynchronous Aloha [5, 6].

This paper focuses on the use of a Low Earth Orbit (LEO) satellite constellation to extend 3GPP LTE NB-IoT. More information about the system can be found in [2] and [3], but this study can be adapted to terrestrial systems. In this system, we encounter a TFA scheme. For that matter, [7] refers to the exploitation of this colliding scheme as a challenge for next generation systems.

In order to estimate the performance of such highly interfered system, the derivation of an expression of the Bit Error Rate (BER) and the Packet Error Rate (PER) as a function of the local interference scenario is an attractive alternative to computationally expensive physical layer simulation.

The collision probability depending on the traffic load has been well studied during the last years [5, 6]. The authors specify that with

no Forward Error Control (FEC), the transmissions are considered as failed when a collision occurs.

Nowadays, in most systems, FEC techniques are used to improve the system performance. In [8], a TFA scheme is studied under several low-rate coding rates, improving the system throughput. Though, the authors do not provide an abstraction method to derive PER estimations: the results are computed via simulations.

In [9], an interesting and simple abstraction is proposed. The paper aims to model first-order performance for any TFA system. The packet error probability is computed independently of the physical layer implementation, and relies on an estimation of an equivalent Signal-to-Interference-plus-Noise Ratio (SINR), depending on all packets lengths and times of arrival. Then, if a relation linking SINR and PER is known, first-order performance can be derived. The authors' method assumes that collisions cause an equivalent white noise, proportionally to the overlapping areas. This implies a symmetric receiver reaction to frequency and time interference.

In [10], a time-only asynchronous Aloha scheme with FEC is assessed, so any collision causes a full frequency overlap. In this case, the interference can be considered as spectrally white. The authors model the behavior of the intra-system interference as an Additive White Gaussian Noise (AWGN), specifying that they believe this approximation to be loose when the number of colliding packets is low.

This paper proposes abstraction methods to compute the BER of a noncoded QPSK transmission, and the PER of a coded QPSK transmission under a TFA access scheme, for a low number of collisions. As described in [2], the transmission follows LTE NB-IoT specifications: both a turbocode and a repetition code spreading are used, as specified by 3GPP in LTE (Release 13) standard [11, 12]. As the interference also follows the same transmission scheme, some common approximations, as whiteness, cannot be used.

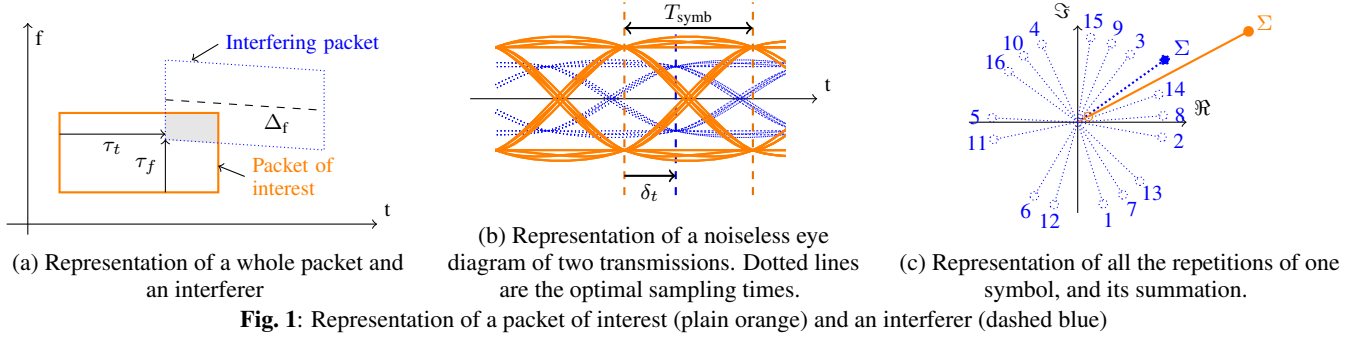
We derive a BER calculation method for a single interferer scenario in section 2, after detailing the parameters used to understand the encountered phenomena.

In section 3, we study the impact of repetition code spreading in TFA schemes, and propose a decoding method.

Finally, we propose an estimation of the PER as a function of any interfering configuration in section 4. This method is adapted from the Mutual Information Effective SNR Mapping (MIESM), mainly used in LTE systems to estimate the PER using several orthogonal subcarriers. Section 5 draws some concluding remarks.

2. WORST CASE BER FOR NON-CODED TRANSMISSION

In this section we estimate the BER of noncoded transmission, of a TFA system. When the number of interfering transmissions is sufficiently high, the resulting interference is well modeled with a normal distribution. When the number of collisions is low, this approximation does not hold anymore. To the best of our knowledge, the BER of noncoded transmission with few intra-system collisions has not been studied yet. In this section, we present an approximation



value of a worst-case BER for a collided transmission plus thermal AWGN, in a single-interferer scenario.

We first consider a Packet of Interest (PoI). For the sake of simplification, we suppose the PoI central frequency to be constantly equal to zero. Let's now consider an interfering transmission. Fig. 1a and 1b present the overlapping parameters linking a PoI (plain orange) and an interferer (dashed blue). In Fig. 1a, τ_t is the normalized time shift (between -1 and 1), τ_f is the normalized frequency shift, and Δ_f is the difference of Doppler rate between the two transmissions. In Fig. 1b, δ_t is the normalized time shift between the optimal sampling times of the PoI and the interferer (between 0 and 0.5).

We first present an approximation value of the best- and worst-case BER for a collided transmission plus thermal AWGN. Then, we mix these models to obtain an approximation for the random case.

As presented in Fig. 1a, when the collision appears, only a part of the PoI is interfered by the collision; we focus on this part of the packet. For the sake of simplification, we consider $\tau_t = 0$.

The k -th symbol of the received signal r can be modeled as:

$$r(k) = A_{\text{PoI}} e_{\text{PoI}}(k) + \alpha_{\tau_f}(k) e_{\text{interf}}(k) + n. \quad (1)$$

A_{PoI} is the received amplitude of the PoI, e_{PoI} and e_{interf} are the emitted QPSK symbols of the PoI and the interferer respectively. Then, r is the received symbol, n is the AWGN and α_{τ_f} is a complex function, representing the interference as a function of τ_f . The packet amplitude is $A_{\text{PoI}} = \sqrt{P_{\text{PoI}}}$, with P_{PoI} the received power of the PoI.

Knowing the behavior of α_{τ_f} as a function of τ_f leads to an estimation of the BER. When δ_t is close to 0.5, the optimal sampling times are separated, we model the resulting interference as an additive white Gaussian equivalent noise. Only a part of the interferer power, noted P_{interf} , goes through the matched filter. The equivalent SNR is calculated as:

$$\text{SNR}_{\text{eq}, 0.5} = \frac{P_{\text{PoI}}/N_0}{1 + (1 - \tau_f)P_{\text{interf}}/N_0} \quad (2)$$

Then, by noting Γ_{BER} the function that estimates the BER as a function of the Signal-to-Noise Ratio (SNR), we obtain the equivalent $\text{BER}_{\text{eq}, 0.5} = \Gamma_{\text{BER}}(\text{SNR}_{\text{eq}, 0.5})$.

When δ_t is close to 0, the reception filter gets matched for the interferer: we observe the BER to be the highest.

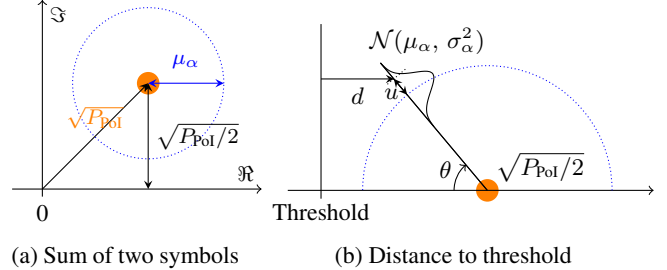
We model α_{τ_f} to be a random variable, with \mathcal{U} the uniform distribution and \mathcal{N} the normal distribution, defined as:

$$\alpha_{\tau_f}(k) = \rho(k) e^{j\phi(k)}, \text{ such as} \quad (3)$$

$$\forall k, \quad \phi(k) \sim \mathcal{U}_{[0, 2\pi]} \text{ and } \rho(k) \sim \mathcal{N}(\mu_\alpha, \sigma_\alpha^2)$$

In our model, the power of the interferer is proportional to the overlapping area, leading to $\mu_\alpha = \sqrt{P_{\text{interf}}(1 - |\tau_f|)}$. We use simulations to approximate the value of σ_α^2 as a function of τ_f . This function mainly depends on the used modulation.

Now that the interfering signal is modeled, we compute the probability of getting an error in the decoder. This probability is



calculated as the expected value of the BER over all the possible received symbols. We first calculate, for every possible received symbol r , the distance $d(r)$ to the threshold, as illustrated in Fig. 2. We use a polar coordinate system $r(\theta, \mu_\alpha + u)$, centered in $A_{\text{PoI}}e_{\text{PoI}}$. Fig. 2a illustrates the probabilistic received symbol as being the sum of a PoI symbol (orange dot), and an interfering symbol (mean of the normal distribution in dotted blue). Fig. 2b represents the coordinate system used in the calculation, and the distance d to the threshold is:

$$d(\theta, u) = \sqrt{\frac{P_{\text{PoI}}}{2}} - (\mu_\alpha + u) \cdot \cos(\theta) \quad (4)$$

The probability of r is now described. So, noting $E(\cdot)$ the expected value and using the tail distribution of the normal distribution Q , we compute the equivalent BER as the expected value of the BER of r , $\text{BER}_{\text{eq}, 0} = E[Q(d(\theta, u))]$. The equivalent SNR is calculated as:

$$\text{SNR}_{\text{eq}, 0} = \Gamma_{\text{BER}}^{-1}(\text{BER}_{\text{eq}, 0}), \quad (5)$$

Γ_{BER}^{-1} being the inverse function of Γ_{BER} , defined earlier.

When δ_t is a random value, uniformly distributed between 0 and 0.5 and using (2) and (5), we heuristically model the BER as being:

$$\text{BER}_{\text{eq}} = \Gamma_{\text{BER}}\left(\frac{\text{SNR}_{\text{eq}, 0.5} + \text{SNR}_{\text{eq}, 0}}{2}\right) \quad (6)$$

In Fig. 3, we present the abstraction performance, with $\text{SNR}_{\text{PoI}} = \text{SNR}_{\text{int}} = 0$ dB, for values of τ_f between 0 and 1. When τ_f is close to 0, the interfering transmission is totally overlapping the PoI with the same power, leading to a high BER. Three types of simulations are presented. In blue, the parameter δ_t is fixed to 0.5. In red, the parameter is fixed to 0. As expected, the BER is the highest for $\delta_t = 0$, but the difference can only be perceived when $\tau_f < 0.3$. The green curves represent the simulation and its abstraction when δ_t is uniformly distributed between 0 and 0.5. The simulation seems to validate the proposed abstractions.

3. INTERFERED CODED TRANSMISSION DECODING

Forward Error Control (FEC) is a common way to improve the global throughput of a system. Both a turbo code and a repetition code are used in the system presented in [2]. In this section, we are

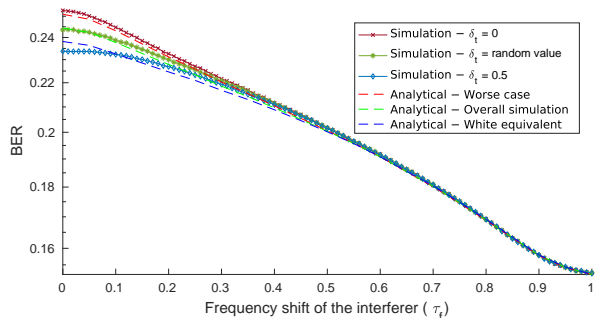


Fig. 3: BER abstraction for equal power PoI and interferer

going to study for this specific satellite system how the repetitions impact the decoding performance.

3.1. Interference analysis

In this system, the repetition coding helps the decoder by adding more diversity to demodulate the messages, but also by lengthening them, in order to simplify the detection and the synchronization. Once the receiver is synchronized with a PoI, the coherent sum of the symbols is transmitted as an input to the turbodecoder.

However, any colliding transmission from the same system is also composed of repetitions. Consequently, the same symbols get summed together, leading hypothetically to an increased interference. Because of the frequency shift, the interferer transmission undergoes a rotation: this phenomena is illustrated in Fig.1c: one PoI and one interferer symbol are represented over all their repetitions, the PoI symbol having a smaller amplitude. Once the summation is performed (displayed as filled dots), we observe that the signal-to-interferer ratio is not only related to the original amplitudes, but also to the frequency rotation between the same symbol of several repetitions. As a result, the summed interferer could be amplified, or reduced, depending on the frequency shift between the PoI and the interferer.

In a terrestrial use of 3GPP standards, a scrambling should prevent this phenomena. The scrambling is performed by multiplying every repetition by a gold code, parameterized for each repetition by the frame number, the first slot number, a ID number of the cell, and an ID number of the terminal (see section 10.1.3.1 of [11]). Because of the frame numbering, the scrambling parameters will loop every 320 ms. By using 3.75 kHz subcarrier, 16 repetitions and 2 Resource Units by repetition as in [2], the scrambling is reinitialized to the same sequence every 5 repetitions, as displayed in Table 1. In this table, the scrambling parameters are presented as a function of the repetition number n_{rep} . A repetition lasts 64 ms; a frame lasts 10 ms, and contains 5 slots, numbered from 0 to 4, as 3.75 kHz subcarriers are used. The frame number is calculated as $n_f = n_{f,\text{init}} + \lfloor (n_{\text{rep}} - 1) \times 6.4 \rfloor$. The slot number is calculated as $n_s = 2 \times (n_{f,\text{init}} + 10 \text{ frac}((n_{\text{rep}} - 1) \times 6.4)) \bmod 5$, where $\text{frac}(\cdot)$ is the fractional part. The table is filled with initial values for frame and slot number equal to 0. We can observe that the sixth repetition follows the same scrambling as the first one. So the phenomena that we presented earlier is reduced by 3GPP scrambling as it is, but not fully prevented.

3.2. Decoding method

In order to decode a transmission, a sufficiently good channel estimation is needed. However the interfering power varies during the PoI reception, making the estimation more complex. As the demodulation is performed after the synchronization in [2], we suppose that the receiver is synchronized with the PoI. The noise power and PoI power are known. In order to improve the signal turbodecoding, we want to estimate the impact of the interfering transmissions on the

Table 1: Example of gold code parameters for a transmission.

Repetition number n_{rep}	1	2	3	4	5	6	7	8
Frame number n_f	0	6	12	19	25	30	36	42
$n_f \bmod 2$	0	0	0	1	1	0	0	0
First slot number n_s	0	3	1	4	2	0	3	1
$\lfloor n_s/2 \rfloor$	0	1	0	2	1	0	1	0

PoI after the summation. The input of the turbodecoder is the likelihood ratio of the summed symbols. No scrambling is used in this section.

In order to sum the repetitions, a classic method is to use a Maximum Ratio Combining (MRC) [13]. In this method, we multiply each repetition m by a weighting factor ρ_m , in proportion to the signal-to-noise ratio, before the summation. Evaluated in [14], this method proposes the best result for diversity combining for a collision free Viterbi decoding. However, as presented in the previous section, knowing the power of an interfering transmissions is not sufficient enough to estimate the signal to interferer power ratio.

We compare several summation methods to decode the interfered transmissions.

- Unweighted** summation. All the weighting coefficients are equal, and depend on the estimated power of the PoI. We present PER performance for perfectly estimated power (O.U., for Oracle Unweighted), and a realistic estimation of the power (R.U., for Realistic Unweighted), using the pilot symbols.
- Maximum Ratio Combining** summation, without knowledge on the interfering summation.
- Optimization solving** summation. We propose to solve an optimization problem, which consists in minimizing the power that is not the PoI signal. Let $\rho = [\rho_m]$ be the weighting vector, and A_{PoI} the amplitude of the received PoI. The total power of the interfered transmission $P_{\text{tot}}(\rho)$ is easily estimated. The PoI power is:

$$P_{\text{PoI, sum}}(\rho) = \left(\sum_{m=1}^{N_{\text{rep}}} \rho_m A_{\text{PoI}} \right)^2 \quad (7)$$

We solve the following optimization problem:

$$\rho_{\text{opti}} = \underset{\rho}{\text{argmin}} P_{\text{tot}}(\rho) - \left(\sum_{m=1}^{N_{\text{rep}}} \rho_m A_{\text{PoI}} \right)^2 \quad (8)$$

We use simulations to compare those three methods. We first generate a set of random configurations, with one interferer. The transmission parameters, i.e. power, Doppler shift, drift of the PoI and the interferer, follow the same distributions as presented in [2], and correspond to NB-IoT devices received by a LEO satellite. The terminals send their transmission over $N_{\text{rep}} = 4$, or 8 repetitions, and using a transmitting power $P_{T_X} = 15$, or 23 dBm. For each configuration, we measure a PER for every summation method. The average PER is presented in Table 2. The MRC summation does not provide the best result, because it tends to drop the interfered parts, leading to a lack of information to decode the transmission.

Table 2: Decoding performance of summation methods.

Simulation parameters			Performance (PER)			
N_{interf}	N_{rep}	P_{T_X}	R.U.	O.U.	MRC	Optim.
1	4	23 dBm	0.01	0.01	0.13	0.01
1	4	15 dBm	0.86	0.86	0.93	0.86
1	8	15 dBm	0.62	0.57	0.70	0.60

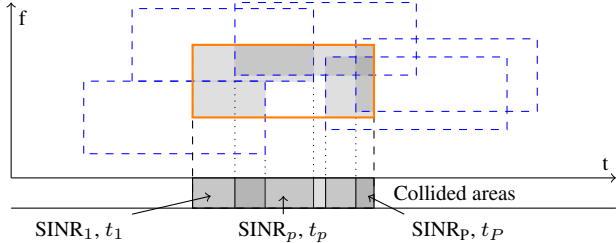


Fig. 4: Representation of the distinct interfered parts (in grey) of a collided PoI (in orange).

The realistic summation method that provides the best result is the optimization-based proposed method. This solution is also the most computationally demanding.

4. PER ESTIMATION FOR CODED TRANSMISSION

In [9], the authors propose an abstraction model of the lower layer in order to speed up a whole system simulation. In this section, we propose a novel abstraction method to estimate the Packet Error Rate (PER) of a given collided scenario, and compare it to abstraction proposed in [9] for TFA schemes. The proposed method is not symmetrical in the time and frequency domains, and relates on a the Mutual Information of each temporal part of the transmission.

4.1. Proposed abstraction method

The abstraction is inspired from Mutual Information Effective SNR Mapping (MIESM), as described in [15].

In a specific scenario, we know the parameters of the colliding transmissions. We know the power P_{interf}^i and the parameters τ_r^i , and τ_t^i of the interfering transmission i , as previously defined, and represented in Fig. 1. We also know the power of the PoI P_{PoI} , and the AWGN power N_0 . Let P be the number of areas defined by $P - 1$ interferers. In Fig. 4, we represent these areas for $P = 6$. For each area p , we compute a relative duration t_p of the area (such as $\sum_p t_p = 1$), and we compute a SINR:

$$\text{SINR}_p = \frac{P_{\text{PoI}}}{N_0 + \sum_{i=1}^{N_{\text{interf}}} \delta(p, i)(1 - \tau_r^i)P_{\text{interf}}^i} \quad (9)$$

The function $\delta(p, i)$ is equal to 1 if the interferer i is received during area p , and 0 otherwise. For most real world collided scenarios, and with a sufficient scrambling between repetition (at least as defined in the previous section), we believe that considering the intra-system interference as a Gaussian noise is a sufficient approximation to estimate the PER.

Then, the proposed method relies on mutual information. Instead of considering the channel as a single interfered channel, we consider the transmission to be distributed over P channels, with different SINR, and we combine the channels by using the following formula:

$$\text{SNR}_{\text{eq}} = \beta_1 I^{-1} \left(N_{\text{rep}} \sum_{p=1}^P t_p I \left(\frac{\text{SINR}_p}{\beta_2} \right) \right) \quad (10)$$

I is the mutual information for a QPSK constellation, and I^{-1} is its inverse function. This function can be computed easily and only depends on the constellation. However, the calibration parameters β_1 and β_2 are fixed by simulations without any intra-system interference, and depend on the coding rate and the number of repetitions.

Using interference-free simulations, we can interpolate the PER curve as a function of the SNR for a AWGN channel, $\Gamma(\text{SNR})$. Then, the β parameters are calibrated in order to minimize the error between the PER of the simulation and the estimated PLR without interference given by $\Gamma(\text{SNR}_{\text{eq}})$.

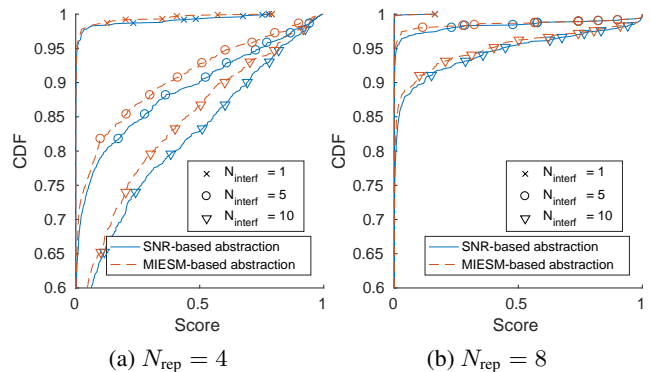


Fig. 5: Performances of the abstraction methods.

4.2. Results

In order to estimate the performance of the estimation of the PER, we define a score, that measures the difference between the simulated PER and the estimated PER.

We aim to model first-order system performance, so the whole system transmission loss target is around 10 %, as proposed in [2]. The score has been chosen to favor correct coarse estimations of the PER. For every configuration, the score s is defined as $s = |\text{PER}_{\text{estim}} - \text{PER}_{\text{simu}}|$, taking values between 0 and 1. A score close to 1 means that the packet demodulation probability has been badly estimated. We display in Fig. 5 the Cumulative Density Function (CDF) of this score. The best estimations show a CDF close to 1 for a low score, meaning that most of the collision configurations have been well estimated.

We present the CDF for two methods: the SNR-based abstraction based from [9] (blue), and the proposed MIESM-based abstraction (dashed red). The estimations are compared with different number of repetitions, in order to validate these abstractions for different ranges of SINR. The number of collisions is fixed to 1, 5 and 10.

On the one hand, as expected, the two abstractions propose a good estimation of the PER, especially when the number of collisions is low. When the number of repetitions is higher, the expected PER is close to 0, this is why the two abstractions show good scores.

On the other hand, the proposed abstraction shows slightly better performance than the SNR-based abstraction, especially when the number of repetitions is low. This is due to the importance of knowing the impact of each interferer on every repetition: when the number of repetitions decreases, the importance of each repetition increases in relation to the total number of repetitions. We believe mutual information based methods could lead to more accurate results when the number of collision is low.

Having a good estimation for these moderately loaded scenarios with higher PER is a key feature to propose a relevant sizing of the whole system. Refinements such as taking the Doppler rate into account, should improve the estimation and should be investigated.

5. CONCLUSION

In this paper, we discuss the estimation of BER and PER for transmission following a TFA scheme for coded and noncoded transmission. The focus is made on low number of collisions. We derive a worst-case BER under the case of a single collision for noncoded transmissions. Then we discuss the impact of collisions when using repetitions, such as proposed by 3GPP NB-IoT, on a TFA scheme, and we propose a decoding method that takes into account these repetitions and minimizes the PER. Then, we propose an abstraction of this PER based on mutual information, and compare it to a state-of-the-art SNR-based one; our estimation shows better performance when the number of collisions is low and similar results when the number of collisions is high. This abstraction will be used to estimate the massive number of device the system should accommodate.

6. REFERENCES

- [1] U. Raza, P. Kulkarni, and M. Sooriyabandara, "Low Power Wide Area Networks: An overview," *IEEE Communications Surveys Tutorials*, vol. 19, no. 2, pp. 855–873, Secondquarter 2017.
- [2] S. Cluzel, L. Franck, J. Radzik, S. Cazalens, M. Dervin, C. Baudoïn, and D. Dragomirescu, "3GPP NB-IoT coverage extension using LEO satellites," in *2018 IEEE 86th Vehicular Technology Conference (VTC Spring)*, June 2018, pp. 1–5.
- [3] M. Anteur, V. Deslandes, N. Thomas, and A. L. Beylot, "Modeling and performance analysis of ultra narrow band system for M2M," in *2016 8th Advanced Satellite Multimedia Systems Conference and the 14th Signal Processing for Space Communications Workshop (ASMS/SPSC)*, Sept 2016, pp. 1–6.
- [4] N. Abramson, "The aloha system: Another alternative for computer communications," in *Proceedings of the November 17-19, 1970, Fall Joint Computer Conference*, ser. AFIPS '70 (Fall). New York, NY, USA: ACM, 1970, pp. 281–285. [Online]. Available: <http://doi.acm.org/10.1145/1478462.1478502>
- [5] C. Goursaud and Y. Mo, "Random unslotted time-frequency ALOHA: Theory and application to IoT UNB networks," in *2016 23rd International Conference on Telecommunications (ICT)*, May 2016, pp. 1–5.
- [6] V. Almonacid and L. Franck, "Throughput performance of time- and frequency-asynchronous ALOHA," in *SCC 2017; 11th International ITG Conference on Systems, Communications and Coding*, Feb 2017, pp. 1–6.
- [7] R. De Gaudenzi, O. del Río Herrero, G. Gallinaro, S. Cioni, and P.-D. Arapoglou, "Random access schemes for satellite networks: from VSAT to M2M — A survey," 2016.
- [8] V. Almonacid and L. Franck, "An asynchronous high-throughput random access protocol for low power wide area networks," in *2017 IEEE International Conference on Communications (ICC)*, May 2017, pp. 1–6.
- [9] Z. Li, S. Zozor, J. M. Drossier, N. Varsier, and Q. Lampin, "2D time-frequency interference modelling using stochastic geometry for performance evaluation in Low-Power Wide-Area Networks," in *2017 IEEE International Conference on Communications (ICC)*, May 2017, pp. 1–7.
- [10] R. D. Gaudenzi, O. del Río Herrero, G. Acar, and E. G. Barrabs, "Asynchronous Contention Resolution Diversity ALOHA: Making CRDSA Truly Asynchronous," *IEEE Transactions on Wireless Communications*, vol. 13, no. 11, pp. 6193–6206, Nov 2014.
- [11] *3GPP TS 36.211, LTE; Physical channels and modulation, v.14.3.0*, 3GPP Std., August 2017.
- [12] *3GPP TS 36.212, LTE; Multiplexing and channel coding v.14.4.0*, 3GPP Std., October 2017.
- [13] T. K. Y. Lo, "Maximum ratio transmission," *IEEE Transactions on Communications*, vol. 47, no. 10, pp. 1458–1461, Oct. 1999.
- [14] T. Sakai, K. Kobayashi, S. Kubota, M. Morikura, and S. Kato, "Soft-decision Viterbi decoding with diversity combining," in *Global Telecommunications Conference, 1990, and Exhibition. 'Communications: Connecting the Future', GLOBECOM '90, IEEE*, Dec 1990, pp. 1127–1131 vol.2.
- [15] K. Brueninghaus, D. Astely, T. Salzer, S. Visuri, A. Alexiou, S. Karger, and G. A. Seraji, "Link performance models for system level simulations of broadband radio access systems," in *2005 IEEE 16th International Symposium on Personal, Indoor and Mobile Radio Communications*, vol. 4, Sept 2005, pp. 2306–2311 Vol. 4.